

The damage evolution of 2D-Woven-C/SiC composite under tension loading

Min-ge Duan^{1,2}, Fei Xu^{1,*}, Zhong-bin Tang¹

¹ School of Aeronautics, Northwestern Polytechnical University, Xi'an, 710072, China

² State Key Laboratory of Explosion Science and Technology, Beijing Institute of Technology, Beijing, 100081, China

* Corresponding author: fay.xu@nwpu.edu.cn

Abstract A meso-numerical model is set up to investigate the damage evolution of 2D woven C/SiC based on RVE(representative volume element) because the woven composite has a periodic in-plane structure. Periodic boundary conditions are imposed to the model. Three material models for the fibers, the matrix, and the yarn/matrix interface are considered. Basic damage modes and their evolutions are observed in the simulation. Firstly, the matrix is damaged at the global applied stress around 50Mpa, which agrees well with the tests. The stress/strain relation obtained from the meso-numerical model can represent the behavior of the 2D woven C/SiC under tension loading. Secondly, the void in the matrix plays an important role. The bundle/matrix interface is essential to investigate the interface debonding.

Keywords 2D-C/SiC composites, RVE, damage mechanisms

1. Introduction

C/SiC, as one of the most promising high temperature structural materials for its performance, such as low coefficient of thermal expansion, excellent thermal shock resistance, abrasion resistance, and high specific strength/modulus, has been applied in structures such as air-breathing engines, hot-gas valves and aerospace thermal structures. Consequently, the mechanical properties of the C/SiC has been an active research field for several decades. Both experimental studies and macro- or micromechanical methods have been used to obtain the mechanical properties of the C/SiC^[1-13,20].

In experimental studies, the mechanical characterization of the C/SiC were studied by classical strain measurements, ultrasonic method, AE(acoustic emission) technique, infrared thermography and microstructural observations under the load of uniaxial tension^[1-6], compression^[1,5], in-plane shear^[7], tension fatigue^[8,9], thermal fatigue^[10,11] and low-velocity impact^[12]. Based on the expensive experiments, the damage modes found by microstructural observations are: matrix cracking, transverse bundle cracking, bundle/matrix and inter-bundle debonding, fiber cracking, ply delamination, bundle splitting and matrix wear. The damage evolution or development mention in the former studies are all deduced from the possible damage modes, which can only reflect the overall damage event and the detailed mechanical behavior of the constituents identification is beyond the detection. Fortunately, it is possible to identify detailed mechanical behavior of the constituents in FEM. However, there is not so much study on C/SiC with simulation method as experiment method. The prediction of the stiffness tensor has been carried out with FEM^[13]. While, little work was done on the prediction of damage evolution and the strength^[4].

Recently, simulation of plain woven fabrics based on photomicrograph measurement and idealized sinusoidal representation of the weave structure has been successfully applied to determine their mechanical properties by taking the advantages of their inherent periodicity of woven fabric architecture^[14-19] at mesoscale in-plane. Both elastic moduli^[14,15], damage^[16] and fracture^[18] behavior of the woven fabrics have been successfully predicted for the case of two-phase heterogeneous materials without considering the fiber-matrix interface using FEM by RVE (representative volume elements). While, it has been confirmed that interface obviously has great

influence on the macroscopic behavior, the toughness and strength of CMCs^[20]. Interfaces are very narrow regions between matrix and fibers and are responsible for a variety of key properties, because of its significance role of stress transfer between fibers and matrix^[20-23]. Recently, CZM(cohesive zone model) is being increasingly used in describing interfacial debonding and separation^[23]. It was first proposed to analyze brittle fracture, and developed to model debonding of inclusions, crack growth processes in elastic-plastic solids, delamination process in composites subjected to low velocity impacts and so on. It is not so easy to simulate the bundle/matrix interface, because the mechanical properties of the interface is very difficult to obtain and the geometry of the interface in woven fabrics is curved surface.

The aim of the present contribution is to introduce the interface into the RVE model in terms of CZM, and to analyze the damage evolution in 2D woven C/SiC with the damage behavior of different constituents identified clearly. This paper is organized as follows: firstly, the geometry model and boundary conditions are presented. Next, the meso-model was outlined with the description of material models of matrix, fiber yarns and interface-matrix interface. Then, the damage of different constituents was predicted based on elastic model. In the last but one section, the damage initiation and evolution are described with different damage modes identified. Finally, conclusions are summarized in the final sections.

2. RVE and periodic boundary conditions

2D woven C/SiC is plain weave fabrics, which are formed by weaving of yarns, as shown in Fig. 1. The black yarn are in X(longitudinal) direction and the grey yarn are in Z(transverse) direction.

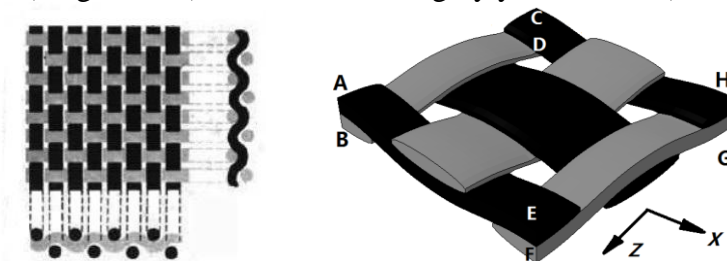


Figure 1. Sketch of 2D plain weave single lamina(left) and its RVE without matrix(right)

In order to modeling the fabric-reinforced laminates using FEM, the representative volume elements (RVE) of the respective configurations are chosen. The RVE is the repeated element that can represent the whole composite fabric structure by a periodical array. Then characteristics of the macrostructure composites can be represented by the RVE with a certain proper boundary conditions. And the data points are fit to a sinusoidal function of the form^[15]:

$$f(x) = a \sin(bx + c) + d \quad (1)$$

where, a, the amplitude of the yarn curve is 0.125mm; $b=2\pi/1.8 \approx 3.49$, and 1.8 is the pitch of the yarn path curve in millimeters; d, the offset depicted is ± 0.125 mm; c is the phase adjusting factor.

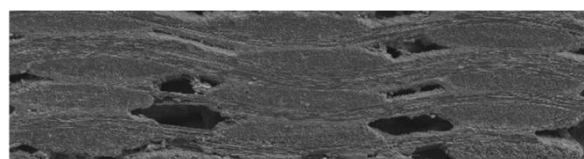


Figure 2. The photomicrograph of the 2D plain weave C/SiC

Fig. 2. is the photomicrograph of the 2D plain weave C/SiC by SEM. According to the micrograph the geometry of the fiber yarns is determined, $AB=0.25\text{mm}$, $AE=AD=1.8\text{mm}$, with the woven hole in the square of $0.2\text{mm} \times 0.2\text{mm}$.

The periodic boundary conditions meets the requirement of displacement periodicity and continuity of the proper boundary conditions, which implies that no separation or overlap will be found between neighboring of RVEs. Each RVE in the composites has the same deformation mode. As stated by Z.Xia^[18], the periodic conditions on the boundary ∂V is

$$u_i = \bar{\varepsilon}_{ik}x_k + u_i^* \quad (2)$$

where, $\bar{\varepsilon}_{ik}$ are the average strains, u_i^* is the periodic part of the displacement components on the boundary surfaces and it is related to the applied global loads. Aboudi has developed a unified micromechanical theory based on the study of interacting periodic cells, and its boundary conditions, plane-remains-plane, were applied to the RVE models in the normal traction loading conditions.

Now based on these the proper boundary conditions are the planes ABFE and CDGH keeps plane during the loading in x direction on EFHG plane. The ABCD plane keeps zero displacement in X direction. And to avoid the rigid motion, the displacement components of the center point of the ABCD plane are assumed to be zero.

3. The meso-model

In the model, RVE that used to investigate the 2D woven C/SiC under tension loading, is shown in Fig. 3. The matrix, fiber and the yarn/matrix interface are taken into account with their specific damage behavior.

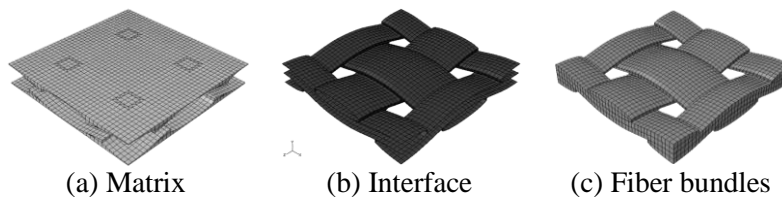


Figure 3. The RVE model and its constituents

3.1. Matrix

The elastic constants for the matrix material SiC: Young's modulus E , Poisson's ratio ν are found to be $E=430\text{Gpa}$, $\nu=0.3$. The brittle cracking material constitutive in ABAQUS is chosen to describe the damage and failure behavior of the isotropic brittle matrix. The failure stress and displacement are 200Mpa and 0.02mm , respectively. In order to consider void in matrix, the elastic constants is assumed to reduced to 10% of the original matrix, and the model with void is shown in Fig. 3(a), the small squares in the RVE is the void region.

3.2. Fiber yarns

The fiber bundles in C/SiC is regarded as transverse isotropic materials. And the properties are listed in Table 1.

Table 1. The mechanical properties of the fiber yarns

$E_1(\text{Gpa})$	$E_2(\text{Gpa})$	ν_{12}	ν_{23}	$G_{12}(\text{Gpa})$	$G_{23}(\text{Gpa})$	$\sigma_f(\text{Mpa})$	ε_f
220	13.8	0.2	0.18	9	4.8	800	1.5%

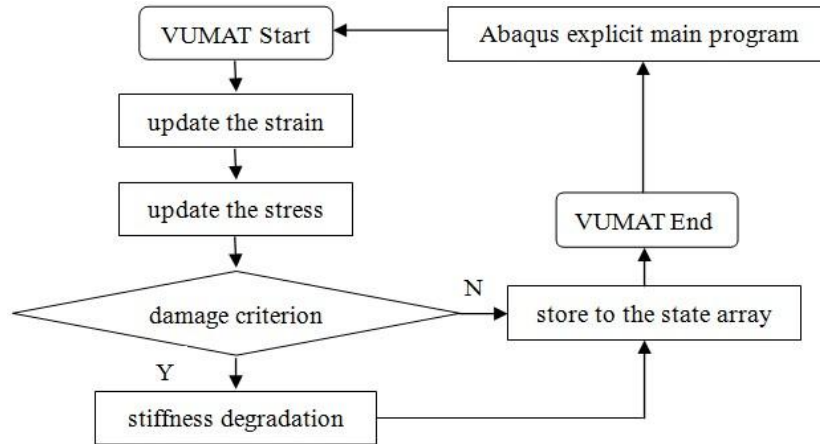


Figure 4. The flow chart for the VUMAT

To study the damage process, the damage model is introduced to the fiber yarns with VUMAT by Fortran, and the flow chart is shown in Fig. 4. Here the maximum stress criterion and linear stiffness degradation are chosen as the damage initiation criterion and damage evolution law of the fiber yarns.

3.3. Yarn/matrix interface

The interface zone plays a key role in the mechanical behavior of composite materials. Its properties can be influenced by different fiber coatings such as PyC, BN or SiC and its thickness. And the most important mechanism for improving the toughness of CMCs is the crack deflection along the interface after the initiation of the matrix cracking. In this meso-level FEM model, the inner-yarn interface is not considered, and fiber bundles is simplified as transversely isotropy.

In this work, bilinear models both for normal and tangential separation is used to simulate the response of the yarn/matrix interfacial zone. The curve of normal and tangential tractions with respect to δ_n and δ_t are shown in Fig.5, where σ_{\max} and τ_{\max} are the interface normal and tangential strength, are 200Mpa and 150Mpa respectively; δ_{\max} is the interface characteristic length parameter; δ_n and δ_t denote the non-dimensional normal and tangential displacement respectively.

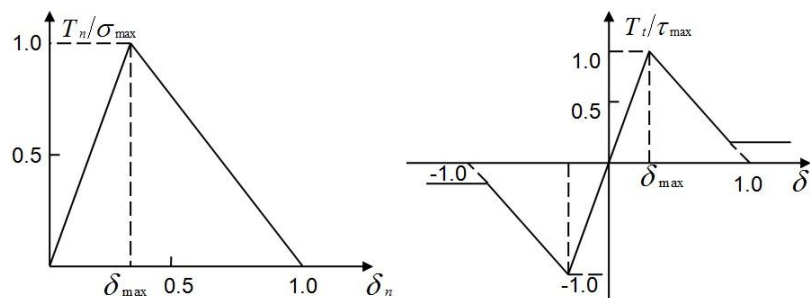


Figure 5. The curve of normal(left) and tangential(right) tractions with respect to δ_n and δ_t

In the FE model, CZM was realized by either cohesive element or cohesive behavior and maximum stress criterion was used to predict the damage initiation in Abaqus/explicit, and detailed constitutive model for the CZM can be found in the help documentation^[24].

4. The result analysis

4.1. The mesh sensibility and validation

Firstly, in order to get accurate results, the mesh sensibility was studied with mesh size 10um, 30um and 50um in the quarter model. The result of the overall force-displacement response and the mises contour are shown in Fig.6. The overall force-displacement response shows very small difference. The mises contour pictures corresponding to the loading of 1.12×10^{-3} mm for 10um, 30um and 50um are listed from left to right(white means 0Mpa, and black grey means 200Mpa, and black means exceeding 200Mpa), the maximum stress in matrix is between 203.3Mpa and 208.7Mpa, while it is 250.8Mpa and 273.1Mpa for the yarns, which shows little difference. So, 50um was accepted for its time-efficiency.

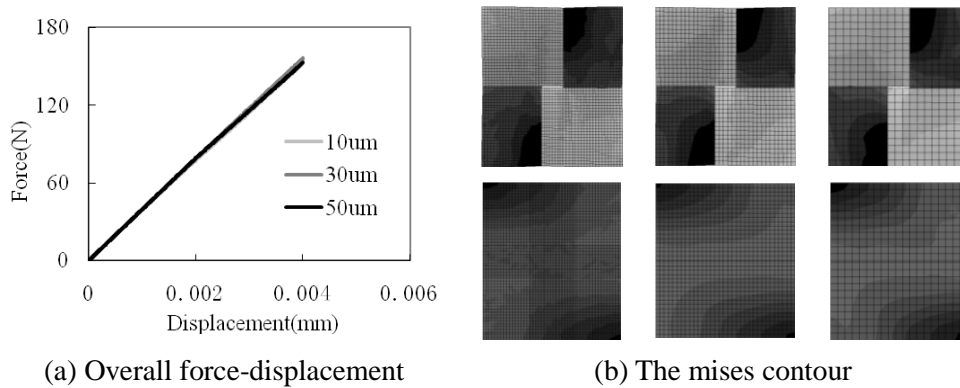


Figure 6. The effect of mesh size

The prediction of the elastic modulus is about 75Gpa. And the elastic modulus from experiments is almost between 70Gpa^[10,11] and 81.2Gpa^[3]. Furthermore, the damage in RVE initiates at the stress about 53Mpa in the matrix, which agrees well with the initial proportional limit of the composites^[3], around 50Mpa.

4.2. The damage prediction

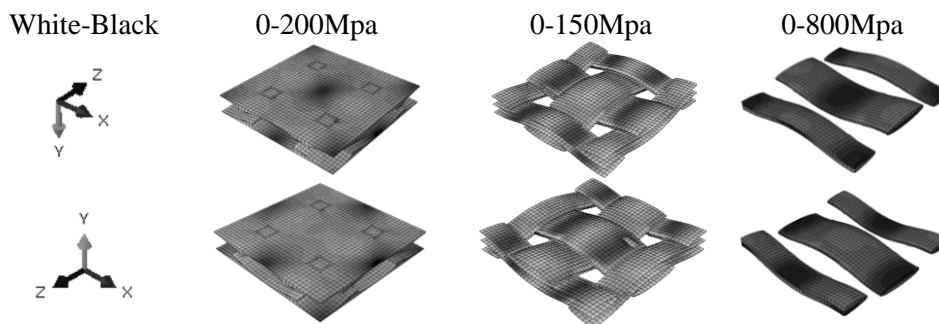


Figure 7. The mises contour of matrix(5th step)/interface/fibers(37th step)

From the elastic RVE model, the matrix is probably damaged first at the thinnest region that close to the yarns, the damage of the yarns will initiate at the woven point, and the interface is easy to get damaged at the region of woven edge, shown in black in Fig. 7.

When the stress in matrix reaches the strength, the average stress in the RVE is about 53Mpa. When the stress in the yarns reaches the strength, the average stress in the RVE is about 330Mpa,

corresponding to strain about 0.005 in Fig. 8 of the grey curve, higher than the failure stress of the composites, which indicates the limitation of the elastic model. So the damage models are introduced to the constituents of the C/SiC, and the corresponding stress-strain curve compared with no damage model is shown in Fig. 8. The detailed damage process of the three constituents are shown in subsequent sections.

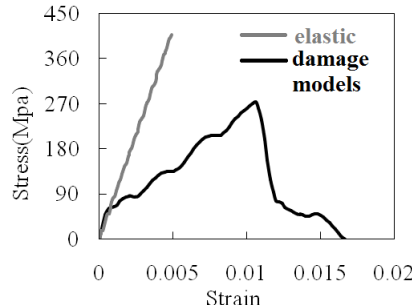


Figure 8. The stress-strain curve

4.3. The matrix damage evolution

The brittle cracking was introduced to matrix for its brittleness in fracture process. Fig. 9 shows the damage initiation and propagation process of the matrix in terms of STATUS, which represents the state of the element (1.0 means the element is active, shown in white; and 0.0 means the element is inactive, shown in black). It is found that the damage first occurs at the thinnest region close to the yarns in loading directions as predicted in the elastic model. In the upper(Y+) matrix, the damage initiates at the edge center of the RVE, while in the lower(Y-) matrix, it initiates at the center of the RVE. Then, the damage propagates in Z direction, vertical to loading. And the damage first runs through the Z direction in the lower matrix at the strain of $2200\mu\epsilon$, while it happens to the upper matrix at the strain of $2600\mu\epsilon$. The damage has already run through the cross section of the RVE at the strain of $2600\mu\epsilon$.

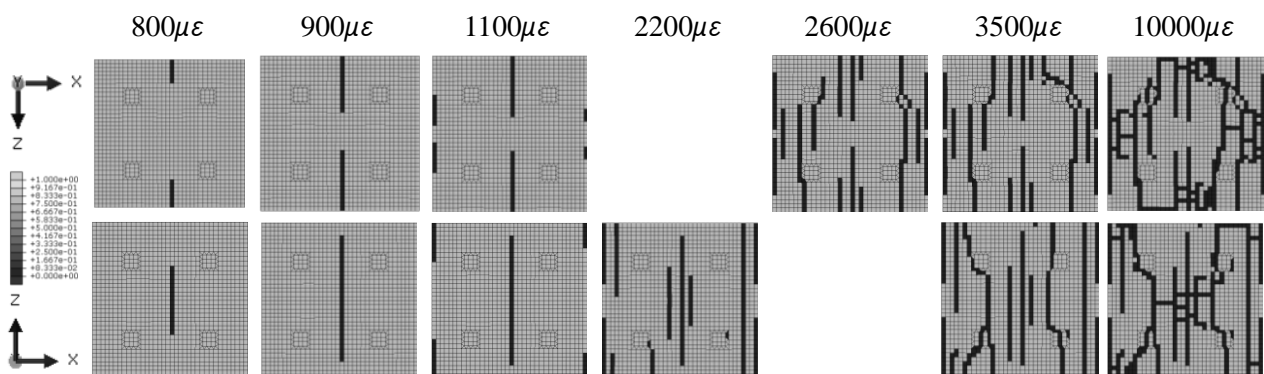


Figure 9. The damage process of the matrix

4.4. The fiber damage evolution

The simulation of fiber damage was introduced by VUMAT in Abaqus, which aims at investigating the possible damage process of fiber bundle damage. Fig. 10 shows the damage initiation and propagation process of the matrix in terms of STATUS. It is found that the damage first occurs at the weaving center of the yarns in loading directions as predicted in the elastic model. Then, the damage propagates in Z direction, vertical to loading. And the damage first runs through the Z direction in longitudinal yarns at the strain of $5800\mu\epsilon$, while it happens to the center yarns in

longitudinal at the strain of $6000\mu\epsilon$.

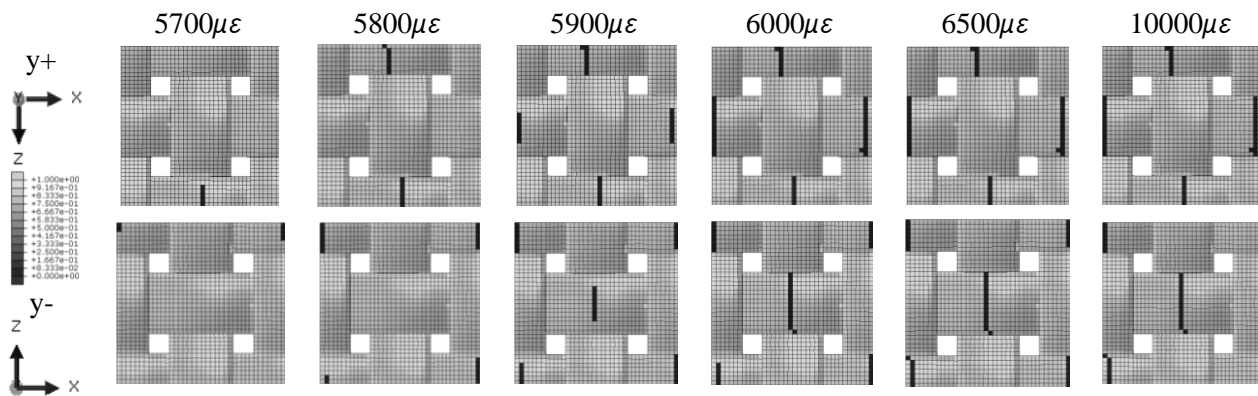


Figure 10. The damage process of the fiber bundle

4.4. The yarn/matrix interface damage evolution

The CZM was introduced to the RVE by cohesive element in Abaqus, which aims at investigating the possible damage process of yarn/matrix interface.

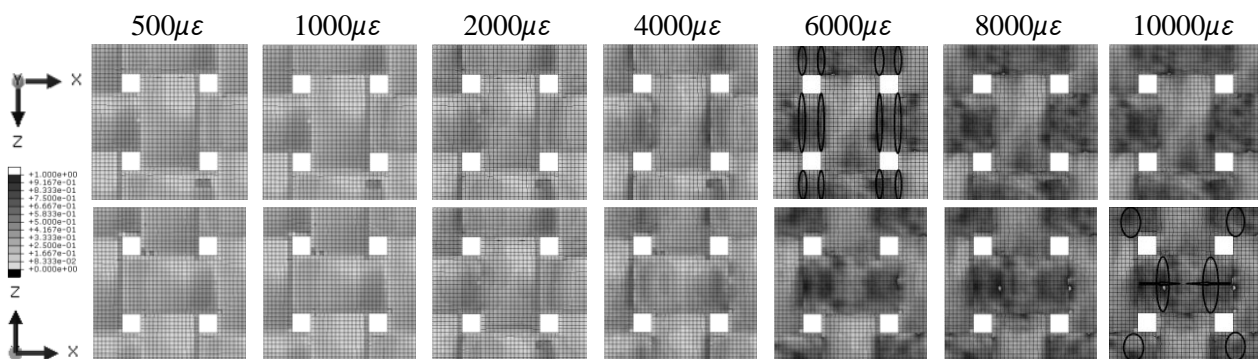


Figure 11. The damage process of the interface

Fig. 11 shows the damage initiation and propagation process of the interface in terms of MAXSCRT (0.0 means no damage occurs, shown in white grey; and 1.0 corresponding to failure, shown in black grey). It is found that the damage initiates at the weaving edge of the interface around the yarns in longitudinal direction as shown in the MAXSCRT contour of $6000\mu\epsilon$, then it spread to the weaving point of the RVE in longitudinal(X) direction, marked with circles and arrows. The interface around yarns in transverse(Z) direction get damaged at the strain of $10000\mu\epsilon$, later than it in longitudinal direction.

4.6. The effect of the void in matrix

The porosity in C/SiC may have great influence on the damage initiation, evolution. So, the RVE with void in matrix is investigated. From the photomicrograph of the 2D plain weave C/SiC, it can be found that the void in matrix is mainly around the weaving gap between yarns, so the mechanical properties of the matrix in this region, showing as four small rectangles in the matrix (the volume is about 6% of the whole volume of the RVE) is reduced to 10%. The result of the matrix damage evolution is shown below in Fig. 12. The damage of the matrix initiates around the void, which differs from the damage evolution in matrix without void compared with Fig. 8. And it is also found that the through damage in the model with void comes earlier than that without void. So the void in

matrix plays an important role in the damage evolution.

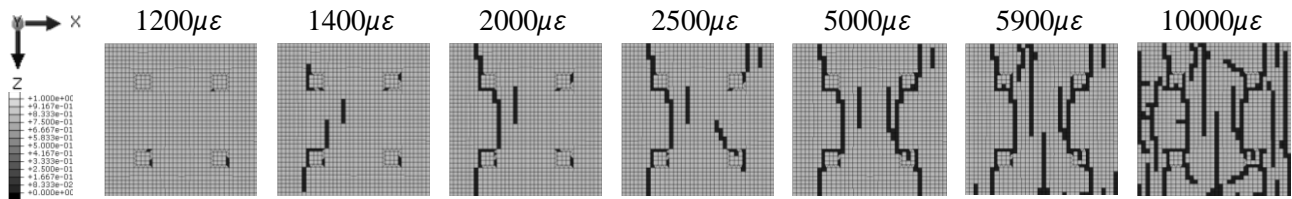


Figure 12. The damage process of the matrix with void

5. Conclusions

This paper focuses on the 2D plain woven C/SiC, and the conclusions are as follows:

- 1) The geometry model of RVE is established based on the photomicrograph of the 2D plain weave C/SiC by SEM with the yarn/matrix interface successfully introduced. And the damage models for the matrix, yarn/matrix interface and yarns are considered.
- 2) The established meso-level FEM is able to describe mechanical behavior of different constituents in the plain-woven C/SiC. Especially, the damage initiates in the matrix at the overall stress about 50Mpa, which agrees well with the experiments.
- 3) The damage of the matrix initiates near the void and spreads in transverse directions, and spreads through the section of the RVE; the damage of the fiber begins at the very region of the weaving point in longitudinal yarns and spreads in transverse direction; the damage of the yarn/matrix occurs near the weaving edge and spreads both in transverse and longitudinal directions.
- 4) The void in the matrix has great influence on the damage initiation and evolution of the matrix in the RVE model. It is found that the damage of the matrix without void initiates near the yarn in Z direction at the thin region of the matrix, while the damage of the matrix with void initiates around the void.

Acknowledgements

This work is supported by the Open Foundation provided by the State Key Laboratory of Explosion Science and Technology (KFJJ12-14M), the Natural Science Foundation of China (90916027), and the Natural Science Fund for Young Scholars of China (11102168).

References

- [1] C. Gerald, G. Laurent, B. Stephane, Development of damage in a 2D woven C/SiC composite under mechanical loading: I. mechanical characterization. *Composites Science and Technology*, 56 (1996) 1363–1372.
- [2] E.B. Rachid, B. Stephane, C. Gerald, Development of damage in a 2D woven C/SiC composite under mechanical loading: II. ultrasonic characterization. *Composites Science and Technology*, 56 (1996) 1373–1382.
- [3] M. Hui, L.F. Cheng, L.T. Zhang, Y.D. Xu, Z.X. Meng, C.D. Liu, Damage evolution and microstructure characterization of a cross-woven C/SiC composite under tensile loading. *Journal of the Chinese ceramic society*, 35 (2007) 137–143. (in Chinese)
- [4] C.P. Yang, G.Q. Jiao, B. Wang, Tensile damage behavior of 2D-C-SiC composite. *Journal of Aeronautical Materials*, 30 (2010) 87–92. (in Chinese)
- [5] G.Y. Guan, G.Q. Jiao, Z.G. Zhang, Uniaxial macro-mechanical property and failure mode of a 2D-woven C/SiC composite. *Acta Material Composite Sinica*, 22 (2005) 81–86. (in Chinese)
- [6] M.D. Wang, C. Laird, Characterization of microstructure and tensile behavior of a cross-woven C-SiC composite. *Acta mater*, 44 (1996) 1371–1387.

- [7] G.Y. Guan, G.Q. Jiao, Z.G. Zhang, In-plane shear fracture characteristics of plain-woven C/SiC composite. *Mechanical Science and Technology*, 24 (2005) 515–521.(in Chinese)
- [8] M.D. Wang, C. Laird, Tension-tension fatigue of a cross-woven C/SiC composite. *Material Science and Engineering*, A230(1997) 171–182.
- [9] C.D. Liu, L.F. Cheng, X.G. Luan, B. Li, J. Zhou, Damage evolution and real-time non-destructive evaluation of 2D carbon-fiber/SiC-matrix composites under fatigue loading. *Material Letters*, 62 (2008) 3922–3924.
- [10] M. Hui, L.F. Cheng, L.T. Zhang, X.C. Luan, J. Zhang, Behavior of two-dimensional C/SiC composites subjected to thermal cycling in controlled environments. *Carbon*, 44 (2006) 121–127.
- [11] M. Hui, L.F. Cheng, Damage analysis of 2D C/SiC composites subjected to thermal cycling in oxidizing environments by mechanical and electrical characterization. *Material Letters*, 59 (2005) 3246–3251.
- [12] L.J. Yao, Z.S. Li, Y.Q. Cheng, X.Y. Tong, Damage behavior of 2D C/SiC composites under low velocity impact. *Journal of Inorganic Materials*, 25(2010)311-314. (in Chinese)
- [13] Y.J. Chang, Study on damage constitutive model and mechanical properties of C/SiC composite. PhD thesis, Northwestern Polytechnical University, Xi'an, 2008. (in Chinese)
- [14] E.J. Barbero, J. Trovillion, J.A. Mayugo, K.K. Sikkil, Finite element modeling of plain weave fabrics from photomicrograph measurement. *Composites Structures*, 73 (2006)41–52.
- [15] E.J. Barbero, T.M. Damiani, J. Trovillion, Micromechanics of fabric reinforced composites with periodic microstructure. *International Journal of Solids and Structures*, 42 (2005) 2487–2504.
- [16] E.J. Barbero, P. Lonetti, K.K. Sikkil, Finite element continuum damage modeling of plain weave reinforced composites. *Composites: Part B*, 37 (2006)137–147.
- [17] H. Ismar, F. Schroter, F. Streicher, Modeling and numerical simulation of the mechanical behavior of woven SiC/SiC regarding a three-dimensional unit cell. *Computational Materials Science*, 19 (2000) 320–328.
- [18] S.I. Haan, P.G. Charalambides, M. Suri, A specialized finite element for the study of woven composites. *Computational Mechanics*, 27 (2001) 445–462.
- [19] Z. Xia, Y. Zhang, F. Ellyin, A unified periodic boundary conditions for representative volume elements of composites and applications. *International Journal of Solids and Structures*, 40 (2003) 1907–1921.
- [20] J.F. Despres, M. Monthieux, Mechanical properties of C/SiC composites as explained from their interfacial features. *Journal of the European Ceramic Society*, 15 (1995) 209–224.
- [21] R.R. Naslain, The design of the fiber-matrix interfacial zone in ceramic matrix composites. *Composites: Part A*, 29A (1998) 1145–1155.
- [22] P.C. Yang, G.Q. Jiao, Effects of interface on tensile properties of fiber reinforced ceramic matrix composite. *Acta Material Composite Sinica*, 27 (2010) 116–121. (in Chinese)
- [23] N. Chandra, H. Li, C. Shet, H. Ghonem, Some issues in the application of cohesive zone models for metal-ceramic interfaces. *International Journal of Solids and Structures*, 39 (2002) 2827–2855.
- [24] ABAQUS documentation.